# Modeling and Stability Analysis for Multiple Parallel Grid-Connected Inverters System

Xiaoming Zou, Xiong Du, Guoning Wang
State Key Laboratory of Power Transmission Equipment &
System Security and New Technology
Chongqing University, Chongqing, 400044, China
Email: duxiong@cqu.edu.cn

***Abstract*—The Phase-Locked Loop (PLL) plays an important role in stability of three-phase grid-connected inverter system. However, the existing literature all neglect the influence of PLL when analyzing the stability of multiple parallel grid-connected inverters system. So this paper builds the model of the system and analyzes the system stability with considering the influence of PLL. Besides, this paper demonstrates that there exist admittance coupling among multiple parallel inverters. Thus, owing to the coupling effect, it can not obtain the multiple parallel grid-connected inverters admittance by accumulating each inverter admittance in parallel directly. Modeling the inverter mutual coupling is presented in this paper. The correctness of the modeling approach and stability analysis are verified by experimental results with RT-LAB.**

***Keywords—Phase-Locked Loop; admittance coupling; multiple parallel inverters; RT-LAB experiment***

## I. INTRODUCTION

The development of distributed generation technology renders many applications of three-phase grid-connected inverter in power system [1]. With the increase in renewable energy generation capacity, inverters are usually paralleled together to meet the system requirement [2]. And the presence of the grid impedance causes the inverter to be coupled with each other, resulting in stability problems [3]. Therefore, it is vital to study the stability of multiple parallel grid-connected inverters system.

In single grid-connected inverter system, the effect of phase-locked loop (PLL) on system stability has been widely reported [4, 5]. Therefore, it is also necessary to consider the influence of PLL to build the model of multiple parallel grid-connected inverters system, so as to accurately analyze the system stability. Many literatures, such as using the method based on system state-space model [3, 6], loop-gain [7, 8], and impedance model [9, 10, 11], have been studied on the stability of multiple parallel grid-connected inverters system. However, these literatures all neglected the influence of PLL.

Considering the influence of PLL, this paper uses the impedance-based method which is convenient for practical implementation to model and analyze the multiple parallel grid-connected inverters system. Mostly, this paper further demonstrated that the single inverter admittance is coupled with each other in the multiple parallel grid-connected inverters system. Thus the admittance of single inverter can not be directly summed to obtain the admittance of multiple parallel grid-connected inverters. This finding is different from the conclusion in existing literature [9,10].

This work was supported by the National Natural Science Foundation of China under Grant 51577020.

## II. ADMITTANCE MODEL OF SINGLE GRID-CONNECTED INVERTER

In order to model and analyze the multiple parallel grid-connected inverters system, this paper establishes the admittance of single grid-connected inverter firstly. Then, the admittance model is verified through simulation.

### *A. Admittance Modeling of Single Grid-Connected Inverter*

The multiple parallel grid-connected inverters system considered in this paper is depicted in Fig. 1. In the figure, the topology of each inverter is the same, which is shown as Fig. 2. The inverter dc side is connected to the constant voltage source, and three-phase ac side is connected to the same Point of Common Coupling (PCC) of the grid.

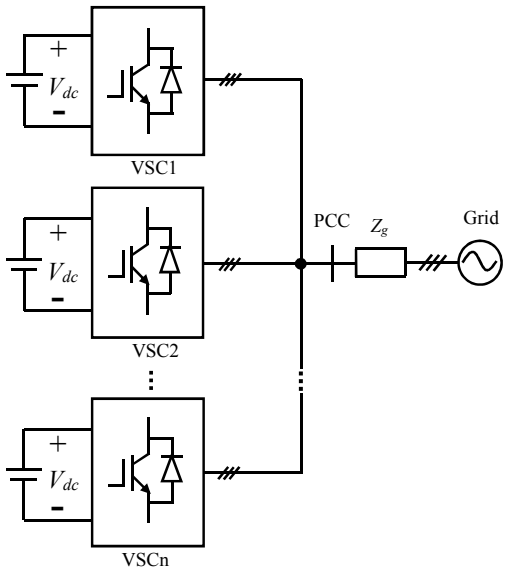


Fig. 1. Multiple parallel grid-connected inverters system.

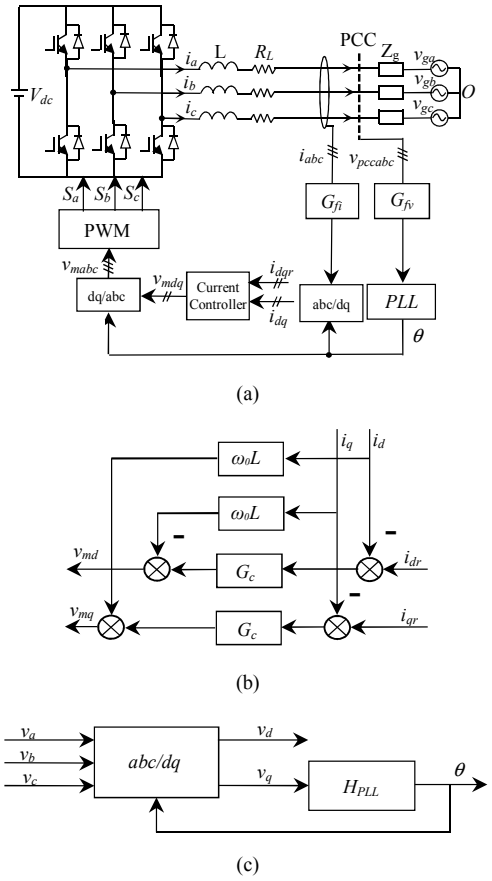


Fig. 2. Single three-phase grid-connected inverter system. (a) The structure of the system. (b) The structure of current controller. (c) The structure of PLL.

In the Fig. 2(a), the grid ideal voltages are denoted as $v_{ga}$, $v_{gb}$, and $v_{gc}$, while the grid impedance as $Z_g$. The voltage at PCC is represented as $v_{abc}$. $G_{fv}$ and $G_{fi}$ represents the transfer function of the sampling circuit for voltage and current respectively. Fig. 2(b) shows the structure of current controller. Fig. 2(c) depicts the structure of PLL.

$G_{fv}$, $G_{fi}$, $G_c$ and $H_{PLL}$ (shown in Fig. 2) can be written as follows:

$$G_{fv}(\omega) = \frac{1}{j\omega\tau_{fv}+1} \tag{1}$$

$$G_{fi}(\omega) = \frac{1}{j\omega\tau_{fi}+1} \tag{2}$$

$$G_c(\omega) = k_p + \frac{k_i}{j\omega} \tag{3}$$

$$H_{PLL}(\omega) = \frac{1}{j\omega}\left(k_{pp} + \frac{k_{pi}}{j\omega}\right) \tag{4}$$

$\tau_{fv}$ and $\tau_{fi}$ represents the sampling interval; $k_p$ and $k_i$ denotes the proportion parameter and integral parameter of current controller respectively; $k_{pp}$ and $k_{pi}$ is the proportion parameter and integral parameter of PLL respectively.

As stated in [4], an input voltage of the inverter at the frequency $\omega_p$ will result in an output current at frequency $\omega_p$ and another output current at frequency $2\omega_0 - \omega_p$. Thus two admittance models $Y_{SA}$ and $Y_{AA}$ are derived to characterize the relationship between voltage at frequency $\omega_p$ and current at frequency $\omega_p$, $2\omega_0 - \omega_p$.

The modeling is achieved by injecting a small signal symmetrical perturbation voltage $\mathbf{V}_{p,\omega_p}$ at frequency $\omega_p$ into the ac side of inverter. First, referring to [4], the small signal model of Park transformation can be expressed as

$$\mathbf{X}_{pdq,\omega_p-\omega_0} = \mathbf{X}_{p,\omega_p} - 0.5\mathbf{X}_{dq}T_{PLL}(\omega_p - \omega_0)\mathbf{V}_{p,\omega_p} \tag{5}$$

$$\mathbf{X}_{pdq,\omega_0-\omega_p} = \mathbf{X}_{p,2\omega_0-\omega_p} + 0.5\mathbf{X}_{dq}T_{PLL}(\omega_0 - \omega_p)\mathbf{V}^*_{p,\omega_p} \tag{6}$$

where $\mathbf{X}_{p,\omega_p}$ and $\mathbf{X}_{p,2\omega_0-\omega_p}$ can be phasors of the perturbation voltage, or the current, the duty ratio, and so on. $\mathbf{X}_{pdq,\omega_p-\omega_0}$ and $\mathbf{X}_{pdq,\omega_0-\omega_p}$ are the corresponding phasors in dq domain. $\mathbf{X}_{dq}$ is the corresponding phasor at fundamental frequency. The PLL can be modeled by

$$T_{PLL}(\omega_p) = \frac{H_{PLL}(\omega_p)}{1+\mathbf{V}_{dq}H_{PLL}(\omega_p)} \tag{7}$$

The small signal model of inverter power stage in phase domain can be expressed as

$$(j\omega_p L + R_L)\mathbf{I}_{p,\omega_p} + \mathbf{V}_{p,\omega_p} = \mathbf{D}_{p,\omega_p}V_{dc} \tag{8}$$

$$\left[j(2\omega_0 - \omega_p)L + R_L\right]\mathbf{I}_{p,2\omega_0-\omega_p} = \mathbf{D}_{p,2\omega_0-\omega_p}V_{dc} \tag{9}$$

where $V_{dc}$ denotes the constant dc bus voltage, $\mathbf{D}_{p,\omega_p}$ and $\mathbf{D}_{p,2\omega_0-\omega_p}$ represent the small signal responses of duty radio.

The small signal models of current controller in dq domain also can be derived at frequency $\omega_p - \omega_0$ and $\omega_0 - \omega_p$, and are shown in (10) and (11) respectively. In (10) and (11), $V_{cr}$ is the amplitude of carrier signal, and $G_d(\omega_p)$ the emulated delay effect.

Combining the models of power stage circuit (8), (9) and current controller (10), (11) through Park transformation model (5), (6), admittance models $Y_{SA}$ and $Y_{AA}$ can be derived as shown in (12) and (13).

$$\mathbf{D}_{pdq,\omega_p-\omega_0} = \frac{1}{2V_{cr}}\left[-\mathbf{I}_{pdq,\omega_p-\omega_0}G_c(\omega_p - \omega_0) + j\omega_0 L\mathbf{I}_{pdq,\omega_p-\omega_0}\right]G_d(\omega_p - \omega_0) \tag{10}$$

$$\mathbf{D}_{pdq,\omega_0-\omega_p} = \frac{1}{2V_{cr}}\left[-\mathbf{I}_{pdq,\omega_0-\omega_p}G_c(\omega_0 - \omega_p) + j\omega_0 L\mathbf{I}_{pdq,\omega_0-\omega_p}\right]G_d(\omega_0 - \omega_p) \tag{11}$$

$$Y_{SA}(\omega_p) = -\frac{\mathbf{I}_{p,\omega_p}}{\mathbf{V}_{p,\omega_p}} = \frac{\frac{1}{j\omega_p L+R_L} - \frac{V_{dc}}{4V_{cr}}\frac{[G_c(\omega_p-\omega_0)-j\omega_0 L]G_d(\omega_p-\omega_0)}{j\omega_p L+R_L}\mathbf{I}_{dqr}T_{PLL}(\omega_p-\omega_0)G_{fv}(\omega_p) - \frac{\mathbf{D}_{dq}V_{dc}}{2(j\omega_p L+R_L)}T_{PLL}(\omega_p-\omega_0)G_{fv}(\omega_p)}{1+\frac{V_{dc}}{2V_{cr}}\frac{[G_c(\omega_p-\omega_0)-j\omega_0 L]G_d(\omega_p-\omega_0)}{j\omega_p L+R_L}G_{fi}(\omega_p)} \tag{12}$$

$$Y_{AA}(\omega_p) = -\frac{\mathbf{I}_{p,2\omega_0-\omega_p}}{\mathbf{V}^*_{p,\omega_p}} = \frac{\frac{V_{dc}}{4V_{cr}}\frac{[G_c(\omega_0-\omega_p)-j\omega_0 L]G_d(\omega_0-\omega_p)}{L(-j\omega_p+j2\omega_0)+R_L}\mathbf{I}_{dqr}T_{PLL}(\omega_0-\omega_p)G_{fv}(-\omega_p)+\frac{\mathbf{D}_{dq}V_{dc}}{2[L(-j\omega_p+j2\omega_0)+R_L]}T_{PLL}(\omega_0-\omega_p)G_{fv}(-\omega_p)}{1+\frac{V_{dc}}{2V_{cr}}\frac{[G_c(\omega_0-\omega_p)-j\omega_0 L]G_d(\omega_0-\omega_p)}{L(-j\omega_p+j2\omega_0)+R_L}G_{fi}(-\omega_p+2\omega_0)} \quad (13)$$

### B. *Admittance Model Verification*

Simulation model of the three-phase grid-connected inverter system shown in Fig. 2 has been built in Matlab/Simulink to verify the accuracy of the admittance models of (12) and (13). The grid impedance $Z_g$ is set to zero. Other parameter values of the simulation model are listed in Table I.

TABLE I. SYSTEM SYMBOLS AND VALUES

| Symbol | Value | Symbol | Value | Symbol | Value |
|---|---|---|---|---|---|
| $v_g$ (rms) | 220V | $k_p$ | 8.83 | $L$ | 1.68mH |
| $i_d$ | 51A | $k_i$ | 386.27 | $R_L$ | 0.15Ω |
| $i_q$ | 38A | $k_{pp}$ | 1.44 | $\tau_{fv}$ | 22.5us |
| $V_{dc}$ | 700V | $k_{pi}$ | 317.22 | $\tau_{fi}$ | 2.2us |

In the simulation, a three-phase symmetrical small-signal perturbation voltage at frequency $\omega_p$ is injected into the grid voltage, and the grid current is extracted. Then the amplitudes and phases of the grid current at $\omega_p$ and $2\omega_0 - \omega_p$ are obtained through FFT analysis. And the amplitude and phase of $Y_{SA}(\omega_p)$ and $Y_{AA}(\omega_p)$ due to the perturbation frequency $\omega_p$ are calculated.

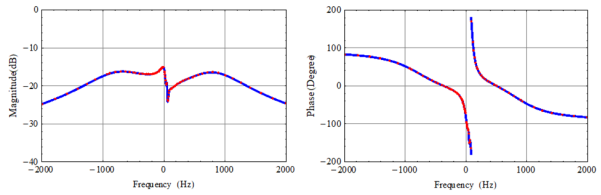


(a) (b)

Fig. 3. Bode plots of the admittance $Y_{SA}(\omega_p)$. Solid line: analytical results; dotted line: simulation results. (a) Amplitude response. (b) Phase response.

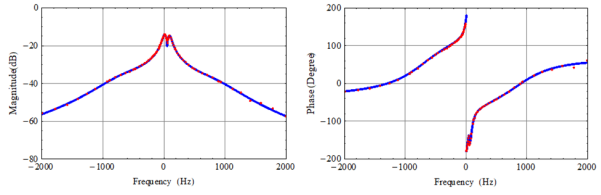


(a) (b)

Fig. 4. Bode plots of the admittance $Y_{AA}(\omega_p)$. Solid line: analytical results; dotted line: simulation results. (a) Amplitude response. (b) Phase response.

Bode plots of the admittance $Y_{SA}(\omega_p)$ are shown in Fig. 3 and the admittance $Y_{AA}(\omega_p)$ in Fig. 4. In both figures, the solid line curves in blue denote the analytical results obtained from (12) and (13), and the dotted line curves in red are the simulation results. It can be seen from Fig. 3 and Fig. 4 that the amplitude and phase characteristics of both admittance models according to (12) and (13) and that from simulation match very well. This verifies the accuracy of single three-phase grid-connected inverter admittance model.

## III. MULTIPLE PARALLEL GRID-CONNECTED INVERTERS SYSTEM

On the basis of establishing single inverter admittance model, the existing literatures [9], [10] directly sum up the single inverter admittance models in parallel to obtain the equivalent admittance model of multiple parallel grid-connected inverters. However, this paper finds that the admittance among inverters in parallel operation are coupled with each other, so the admittance of single inverter can not be directly added to characterize the property of the parallel system. Therefore, in this section, considering the coupling factor among parallel inverters, the admittance model of single grid-connected inverter is modified. Then the stability of multiple parallel grid-connected inverters system is analyzed with the modified admittance model.

### A. *Modification of Single Inverter Admittance Model*

It can be seen from the established admittance model (formula (12) and (13)) that the admittance of the single inverter is closely related to the steady state voltage of PCC. In the multiple parallel grid-connected inverters system, any inverter put into and exiting parallel operation will change the system PCC steady state voltage, and then change the other inverter admittance characteristic. That is the admittance of inverter in parallel operation will be coupled with each other.

Considering the coupling factor among parallel inverters, the PCC steady state voltage in the multiple parallel grid-connected inverter system (as shown in Fig. 1) can be calculated as follows:

$$\mathbf{V}'_{dq} = \sum_{i=1}^{n} \mathbf{I}_{dqri}\,\mathbf{Z}_g + \mathbf{V}_g \quad (14)$$

For the $i$th inverter, the steady state duty ratio $\mathbf{D}'_{dqi}$ can be represented as :

$$\mathbf{D}'_{dqi} = \frac{\mathbf{V}'_{dq}+(j\omega_0 L+R_L)\mathbf{I}_{dqri}}{V_{dc}} \quad (15)$$

And the PLL also can be remodeled by

$$T'_{PLL}(\omega_p) = \frac{H_{PLL}(\omega_p)}{1+\mathbf{V}'_{dq}H_{PLL}(\omega_p)} \quad (16)$$

Based on the formula (14)、(15) and (16), the $i$th grid-connected inverter admittance in parallel system can be modified as (17) and (18).

$$Y'_{SAi}(\omega_p)=\frac{\frac{1}{j\omega_p L+R_L}-\frac{V_{dc}}{4V_{cr}}\frac{[G_c(\omega_p-\omega_0)-j\omega_0 L]G_d(\omega_p-\omega_0)}{j\omega_p L+R_L}\mathbf{I}_{dqri}T'_{PLL}(\omega_p-\omega_0)G_{fv}(\omega_p)-\frac{\mathbf{D}'_{dqi}V_{dc}}{2(j\omega_p L+R_L)}T'_{PLL}(\omega_p-\omega_0)G_{fv}(\omega_p)}{1+\frac{V_{dc}}{2V_{cr}}\frac{[G_c(\omega_p-\omega_0)-j\omega_0 L]G_d(\omega_p-\omega_0)}{j\omega_p L+R_L}G_{fi}(\omega_p)} \quad (17)$$

$$Y'_{AAi}(\omega_p)=\frac{\frac{V_{dc}}{4V_{cr}}\frac{[G_c(\omega_0-\omega_p)-j\omega_0 L]G_d(\omega_0-\omega_p)}{L(-j\omega_p+j2\omega_0)+R_L}\mathbf{I}_{dqri}T'_{PLL}(\omega_0-\omega_p)G_{fv}(-\omega_p)+\frac{\mathbf{D}'_{dqi}V_{dc}}{2[L(-j\omega_p+j2\omega_0)+R_L]}T'_{PLL}(\omega_0-\omega_p)G_{fv}(-\omega_p)}{1+\frac{V_{dc}}{2V_{cr}}\frac{[G_c(\omega_0-\omega_p)-j\omega_0 L]G_d(\omega_0-\omega_p)}{L(-j\omega_p+j2\omega_0)+R_L}G_{fi}(-\omega_p+2\omega_0)} \quad (18)$$

### B. *Stability Analysis of Multiple Parallel Grid-Connected Inverters System*

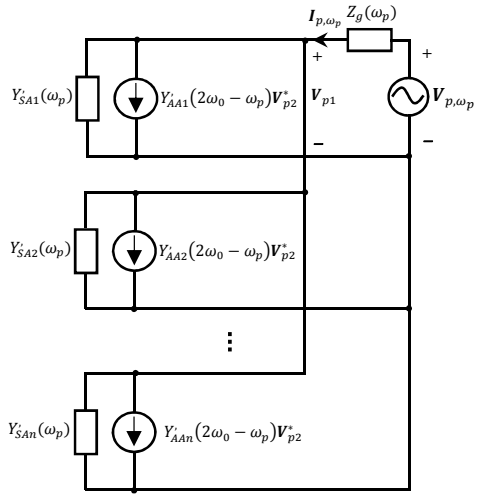


(a)

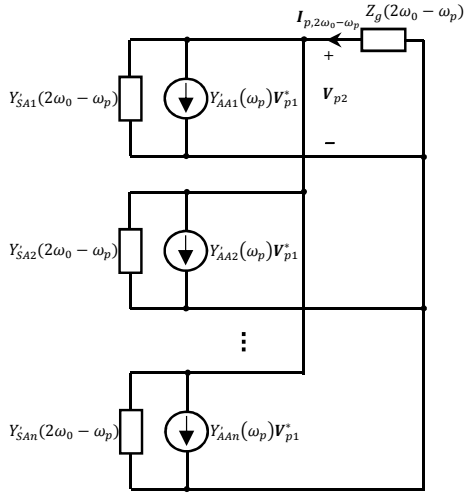


(b)

Fig. 5. Equivalent circuit of multiple parallel three-phase grid-connected inverters system. (a) The equivalent circuit at frequency $\omega_p$. (b) The equivalent circuit at frequency $2\omega_0-\omega_p$.

As mentioned above, for each inverter, the PCC voltage at frequency $\omega_p$ will generate the grid current at frequency $\omega_p$ by $Y'_{SA}$, and the PCC voltage at frequency $2\omega_0-\omega_p$ will also generate the grid current at frequency $\omega_p$ by $Y'_{AA}$. Thus the equivalent circuit of multiple parallel grid-connected inverters system at frequency $\omega_p$ can be represented as Fig. 5(a). Similarly, the equivalent circuit of system at frequency $2\omega_0-\omega_p$ can be represented as Fig. 5(b).

According to the equivalent circuit of multiple parallel three-phase grid-connected inverters system shown in Fig. 5, the system grid current at frequency $\omega_p$ and $2\omega_0-\omega_p$ are as follows:

$$\mathbf{I}_{p,\omega_p}=\sum_{i=1}^{n}Y'_{SAi}(\omega_p)\mathbf{V}_{p1}+\sum_{i=1}^{n}Y'_{AAi}(2\omega_0-\omega_p)\mathbf{V}^*_{p2} \quad (19)$$

$$\mathbf{I}_{p,2\omega_0-\omega_p}=\sum_{i=1}^{n}Y'_{SAi}(2\omega_0-\omega_p)\mathbf{V}_{p2}+\sum_{i=1}^{n}Y'_{AAi}(\omega_p)\mathbf{V}^*_{p1} \quad (20)$$

From above, the equivalent admittance of multiple parallel grid-connected inverters are:

$$Y'_{SAE}(\omega_p)=\sum_{i=1}^{n}Y'_{SAi}(\omega_p) \quad (21)$$

$$Y'_{AAE}(\omega_p)=\sum_{i=1}^{n}Y'_{AAi}(\omega_p) \quad (22)$$

Based on voltage-current relationship shown in (19) and (20), the equivalent inverter admittance matrix of multiple parallel grid-connected inverters system also can be obtained, which is as follows:

$$Y'_{VSCE}=\begin{bmatrix}Y'_{SAE}(\omega_p) & Y'_{AAE}(2\omega_0-\omega_p)\\ [Y'_{AAE}(\omega_p)]^* & [Y'_{SAE}(2\omega_0-\omega_p)]^*\end{bmatrix} \quad (23)$$

Similarly, the grid impedance matrix can be defined as follows:

$$Z_g=\begin{bmatrix}Z_g(\omega_p) & 0\\ 0 & Z_g^*(2\omega_0-\omega_p)\end{bmatrix} \quad (24)$$

Using the equivalent inverter admittance matrix and grid impedance matrix, the stability of multiple parallel grid-connected inverters system can be analyzed with generalized Nyquist criterion (GNC).

## IV. Stability Analysis Results Verification

In this paper, two inverters in parallel operation are considered. The topology and parameters of each inverter are the same. The topology is shown in Fig. 2, and the related parameters are shown in Table I. The grid inductance $L_g$ value is variable.

The GNC plots of $Y'_{VSCE}Z_g$ for the grid inductance of $L_g$ = 3.9mH are shown in Fig. 6. It can be observed from Fig. 6 that both GNC plots do not encircle (-1, 0), which indicates that the system is stable. Experimental results of the multiple parallel grid-connected inverters system are shown in Fig. 7. One can see that the grid currents exhibit no noticeable distortion. As such, the system is stable. This demonstrates that stability analysis result is correct.

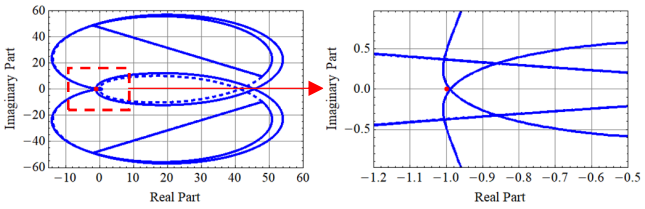


Fig. 6. GNC plots of $Y'_{VSCE}Z_g$ for $L_g$=3.9mH.

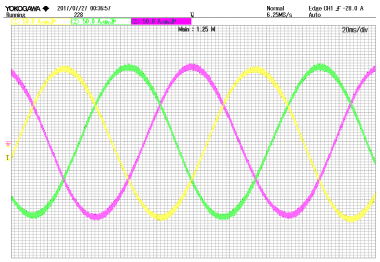

Fig. 7. Waveforms of three phase grid currents for $L_g$=3.9mH.

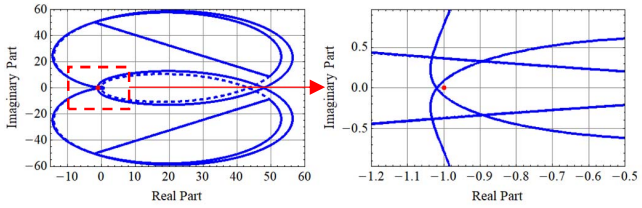


Fig. 8. GNC plots of $Y'_{VSCE}Z_g$ for $L_g$=4.0mH.

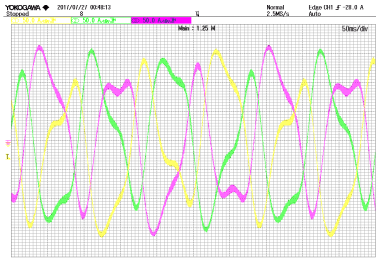

Fig. 9. Waveforms of three phase grid currents for $L_g$=4.0mH.

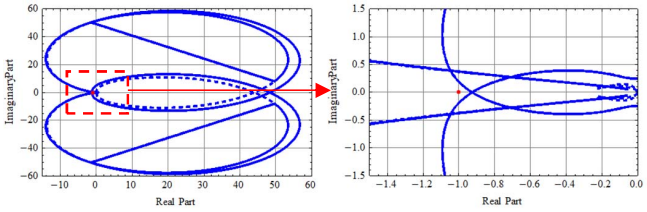


Fig. 10. GNC plots for $L_g$=4.0mH when neglecting the admittance coupling factor.

The corresponding GNC plots of $Y'_{VSCE}Z_g$ are shown in Fig. 8 when the grid inductance $L_g$ is 4.0mH. And one of GNC plots encircles (-1, 0), which implies that the system is unstable. The corresponding experimental results are shown in Fig. 9. It is observed that the grid currents exhibit high degree of distortion, which shows that the system is unstable. So the experimental results verify the correctness of stability analysis result.

For the case that grid inductance is 4.0mH, neglecting the admittance coupling factor among parallel inverters, that means accumulating the admittance of single inverter directly to obtain the equivalent admittance of multiple parallel inverters without modification, the stability of parallel system is reanalyzed. The corresponding GNC plots are shown in Fig. 10 under this circumstances. The GNC plots indicate that the system is stable, that is not consistent with the above analysis and experimental results. So neglecting the inverter mutual coupling factor, the system stability can not be accurately analyzed.

What's more, when the number of parallel running inverter increases, the capacity of grid-connected power increases, and the grid impedance increases, neglecting the admittance coupling factor among parallel inverters will lead greater stability analysis errors.

## V. CONCLUSIONS

This paper built the equivalent admittance model of multiple parallel grid-connected inverters with considering the influence of PLL, which makes up the insufficient of existing literatures. Based on the equivalent admittance model, the stability of the multiple parallel grid-connected inverters can be accurately analyzed.

Mostly, this paper demonstrates that there exist coupling among the inverter admittance in parallel operation, and stability of the multiple parallel grid-connected inverters system can not be accurately obtained with neglecting the admittance coupling factor.

## REFERENCES

[1] F. Blaabjerg, Zhe Chen and S. B. Kjaer, "Power electronics as efficient interface in dispersed power generation systems," *IEEE Transactions on Power Electronics*, vol. 19, no. 5, pp. 1184-1194, Sept. 2004.

[2] F. Blaabjerg, R. Teodrecu, M. Liserre, and Timbus, "Overview of control and grid synchronization for distributed power generation systems," *IEEE Trans. on Ind. Electron.*, vol. 53, no.5, pp. 1398-1409, Oct. 2006.

[3] Y. Wang, X. Wang, F. Blaabjerg, and Z. Chen, "Harmonic instability assessment using State-Space modeling and participation analysis in Inverter-Fed power systems," *IEEE Transactions on Industrial Electronics*, vol. 64, no. 1, pp. 806-816, Jan. 2017.

[4] L. Harnefors, M. Bongiorno and S. Lundberg, "Input-Admittance Calculation and Shaping for Controlled Voltage-Source Converters," *IEEE Transactions on Industrial Electronics*, vol. 54, no. 6, pp. 3323-3334, Dec. 2007.

[5] D. Dong, B. Wen, D. Boroyevich, P. Mattavelli and Y. Xue, "Analysis of Phase-Locked Loop Low-Frequency Stability in Three-Phase Grid-Connected Power Converters Considering Impedance Interactions," *IEEE Transactions on Industrial Electronics*, vol. 62, no. 1, pp. 310-321, Jan. 2015.

[6] Y. Wang, X. Wang, Z. Chen and F. Blaabjerg, "State-space-based harmonic stability analysis for paralleled grid-connected inverters," *in IECON 2016 - 42nd Annual Conference of the IEEE Industrial Electronics Society*, Florence, 2016, pp. 7040-7045.

[7] X. Wang, F. Blaabjerg, M. Liserre, Z. Chen, J. He and Y. Li, "An Active Damper for Stabilizing Power-Electronics-Based AC Systems," *IEEE Transactions on Power Electronics*, vol. 29, no. 7, pp. 3318-3329, July 2014.

[8] M. Lu, X. Wang, P. C. Loh and F. Blaabjerg, "Resonance Interaction of Multiparallel Grid-Connected Inverters With LCL Filter," *IEEE*

*Transactions on Power Electronics*, vol. 32, no. 2, pp. 894-899, Feb. 2017.

[9] C. Wan, M. Huang, C. K. Tse and X. Ruan, "Effects of Interaction of Power Converters Coupled via Power Grid: A Design-Oriented Study," *IEEE Transactions on Power Electronics*, vol. 30, no. 7, pp. 3589-3600, July 2015.

[10] C. Yoon, H. Bai, R. N. Beres, X. Wang, C. L. Bak and F. Blaabjerg, "Harmonic Stability Assessment for Multiparalleled, Grid-Connected Inverters," *IEEE Transactions on Sustainable Energy*, vol. 7, no. 4, pp. 1388-1397, Oct. 2016.

[11] M. Lu, F. Blaabjerg and X. Wang, "Interaction admittance based modeling of multi-paralleled grid-connected inverter with LCL-filter," *2016 IEEE 2nd Annual Southern Power Electronics Conference (SPEC)*, Auckland, 2016, pp. 1-7.